

# Milliseconds microfluidic chaotic bubble mixer

Xiaole Mao · Bala Krishna Juluri · Michael Ian Lapsley ·  
Zackary Stoeri Stratton · Tony Jun Huang

Received: 9 April 2009 / Accepted: 10 August 2009 / Published online: 27 August 2009  
© Springer-Verlag 2009

**Abstract** In this study, we report a rapid microfluidic mixing device based on chaotic advection induced by microbubble–fluid interactions. The device includes inlets for to-be-mixed fluids and nitrogen gas. A side-by-side laminar flow segmented by monodisperse microbubbles is generated when the fluids and the nitrogen are co-injected through a flow focusing micro-orifice. The flow subsequently enters a series of hexagonal expansion chambers, in which the hydrodynamic interaction among the microbubbles results in the stretch and fold of segmented fluid volumes and rapid mixing and homogenization. We characterize the performance of the microfluidic mixer and demonstrate rapid mixing within 20 ms. We further show that bubbles can be conveniently removed from the mixed fluids using a microfluidic comb structure on completion of the mixing.

**Keywords** Chaotic advection · Microbubble · Microfluidics · Rapid mixing

## 1 Introduction

Rapid mixing and homogenization in microfluidic systems (Biddiss et al. 2004; Hardt et al. 2005; Chang and Yang 2007; Miller and Wheeler 2008; Puleo and Wang 2009) is

one of the key obstacles in developing lab-on-a-chip platforms for the studies in chemical kinetics (Pollack et al. 1999) and nanomaterial synthesis (de Mello and de Mello 2004). In order to characterize a rapid biological/chemical process or to achieve optimum synthesis results, reagents must be rapidly mixed before significant progress of the reaction begins to occur. At the micrometer scale, fluidic behavior exhibits low-Reynolds ( $Re$ ) characteristics, such as laminar flow and lack of turbulence, the spontaneous fluctuation of flow field, which allow rapid mixing. Therefore, mixing is limited to the diffusion of the molecules across the fluidic interface between laminar flows (Wu and Nguyen 2005; Mao et al. 2007a, b; Shi et al. 2008; Mao et al. 2009a).

For purely diffusive microfluidic mixing, the species need to diffuse across the entire channel to achieve homogenous mixing. The mixing time,  $t_{\text{mix}}$ , can be estimated from the following equation,  $t_{\text{mix}} = st^2/D$ , where  $st$  is the striation thickness (the distance through which the diffusion must occur) and is approximately equal to the channel width ( $w$ , typically of the order of 100  $\mu\text{m}$ ), and  $D$  is the diffusion coefficient (typically of the order of  $10^{-6} \text{ cm}^2/\text{s}$ ). Therefore, complete mixing by diffusion only in a microfluidic system can take a prohibitively long time ( $\sim 100 \text{ s}$ ). The key to the rapid microfluidic mixing lies in the reduction of  $st$ . Ultrafast micromixing based on hydrodynamic focusing (Knight et al. 1998; Park et al. 2006) has been previously demonstrated for rapid mixing in the milliseconds range by dramatically reducing the  $st$  to micrometer or even sub-micrometer level. Unfortunately, hydrodynamic focusing can only achieve mixing in the focused central stream, limiting its application from homogenizing samples across the entire flow.

Another important approach for rapid microfluidic mixing is chaotic advection (Ottino 1989; Ottino and

---

X. Mao · B. K. Juluri · M. I. Lapsley · Z. S. Stratton ·  
T. J. Huang (✉)  
Department of Engineering Science and Mechanics,  
Pennsylvania State University, University Park, PA 16802, USA  
e-mail: junhuang@psu.edu

X. Mao · T. J. Huang  
Department of Bioengineering, Pennsylvania State University,  
University Park, PA 16802, USA

Wiggins 2004). Chaotic advection causes “stretch and fold” of fluid volumes, giving rise to chaotic fluid particle trajectories even in “smooth” low  $Re$  laminar flow regime and rapid exponential decrease of  $st$  as expressed in  $st(d) = w \times e^{(-\frac{d}{\lambda})}$ , where  $st(d)$  is the striation thickness after the fluid volume has traveled the distance ( $d$ ) along the channel,  $w$  is the channel width (and the initial striation thickness), and  $\lambda$  is a characteristic length determined by the trajectories of the chaotic flow. More importantly, such a rapid decrease of  $st$  occurs in the entire fluidic volume, thus resulting in the rapid homogenization of fluids in the entire flow. A wide variety of mixers based on chaotic advection have been proposed. Three-dimensional geometric obstacles (Stroock et al. 2002; Yang et al. 2005; Floyd-Smith et al. 2006; Kang et al. 2008) or serpentine channels (Liu et al. 2000; Therriault et al. 2003; Schonfeld et al. 2004) have been introduced to induce periodic lateral motion of fluids, leading to the chaotic advection and rapid mixing. However, the complex configuration and fabrication of these 3D microfluidic structures have become limiting factors in their application. Recently, chaotic advection was realized using a much simpler 2D winding channel by periodically shifting the axis of counter-rotating recirculation vortices in moving water-in-oil droplets (Song et al. 2003; Song and Ismagilov 2003). Beyond significantly simplified device geometry, droplet-based chaotic microfluidic mixing can also dramatically reduce sample dispersion since samples are confined in aqueous droplets. However, an apparent disadvantage of droplet-based chaotic mixing is the introduction of an additional organic phase (oil), which may cause complications if further sample purification and analyses are needed.

In light of aforementioned constraints of present chaotic microfluidic mixers, we introduce a microbubble-based rapid microfluidic mixer which is based on rapid chaotic mixing within bubble-segmented fluids. Compared to previously described droplet-based chaotic mixers, microbubble-based mixers provide the same benefit such as simple device geometry and low sample dispersion (Günther et al. 2004; Garstecki et al. 2005; Garstecki et al. 2006). In addition, the separation of gas/liquid phases (Günther et al. 2004) can be conveniently achieved with simple microfluidic structures, which makes it possible to remove the bubbles from the mixed liquids upon the completion of mixing.

## 2 Experimental section

The schematic of the chaotic bubble mixer is shown in Fig. 1. The device includes one inlet for gas (middle) and two inlets for to-be-mixed fluids (upper and lower). A flow focusing orifice (Garstecki et al. 2005) is located at the

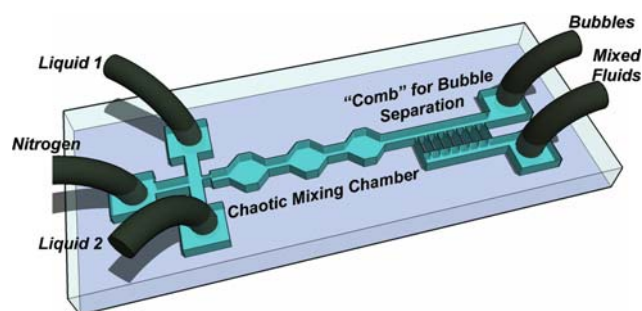


**Fig. 1** Experimental design and setup of the microfluidic chaotic bubble mixer. The device includes inlets for to-be-mixed fluids and gas, mixing chambers in which bubble-induced chaotic mixing occurs and a microfluidic “comb” structure for bubble separation upon the completion of mixing

inlet converging point. The width is  $80 \mu\text{m}$  for all the inlets and the main channel, and  $30 \mu\text{m}$  for the orifice. The depth is  $50 \mu\text{m}$  throughout the device. The device includes a series of hexagonal expansion chambers, in which chaotic mixing occurs. The removal of the bubbles after the completion of mixing is accomplished using a comb-shaped microfluidic structure (Günther et al. 2004). The comb structure includes an additional fluid-extraction branch channel and a series of capillary channels (“comteeth,” width =  $10 \mu\text{m}$ , height =  $50 \mu\text{m}$ ), which connect the branch channel with the main channel. The device was fabricated from polydimethylsiloxane (PDMS) using the standard soft-lithography technique. The silicon mold for the soft lithography was fabricated using deep reactive ion etching (DRIE). The pattern for DRIE was lithographically defined using positive photoresist Shipley 1827. The etching depth on the silicon wafer was set to be  $50 \mu\text{m}$ . Sylgard 184 Silicone Elastomer base and Sylgard 184 Silicone Elastomer curing agent (Dow Corning) were mixed at a 10:1 weight ratio, cast onto the silicon mold, and cured at  $70^\circ\text{C}$  for 2 h. The PDMS device, once peeled from the mold, was drilled with a silicon carbide drill to create the tubular access to inlets and outlets, and subsequently sealed onto a glass slide. Polyethylene tubes were then inserted into the inlets to connect the device with the fluid pump and gas tank. The liquid flow injection was carried out using a syringe pump (KD Scientific 210). The nitrogen inlet was connected with a nitrogen tank, and the gas pressure was controlled via an inline pressure regulator.

## 3 Results and discussion

For mixing, two to-be-mixed solutions, water (top inlet) and ink (waterman black ink, bottom inlet), are co-injected with nitrogen gas at a constant flow rate and pressure through the orifice. Figure 2a depicts the generation of the

bubble-segmented laminar flow and chaotic mixing process. At the orifice, the gas stream breaks into monodisperse microbubbles due to the shearing of the fluids (Garstecki et al. 2005). A clear fluidic interface can be observed between bubbles as the two fluids flow side-by-side in a laminar fashion. The size of the bubble and the filling ratio (the ratio between the volume of the bubble and the volume of segmented fluids) can be adjusted by changing the liquid flow rate and nitrogen pressure (Garstecki et al. 2005).

The mixing occurs when the bubble-segmented laminar flow enters the mixing area—a series of hexagonal expansion chambers (Fig. 2a). On entering the expansion chambers, the bubbles are no longer confined by the channel wall, causing the movements of the bubble to be influenced by neighboring bubbles. At the chamber entrance, the newly arrived bubbles tend to slip to one side of the chamber due to the unsymmetrical pressure field generated by previous bubbles. The system exhibits “oscillation” behavior, which leads the alternative distribution of bubbles into a different side of the chamber. During this process, the segmented fluid volumes, which contain both water and ink, are also alternatively distributed into different portions of the chambers. As bubbles travel through the mixing chamber, they collide with each other (0.1% Triton X-100 surfactant from Sigma-Aldrich was added into both ink and water to avoid the bubble coalescence), constantly changing their relative positions and moving directions. As a result, the segmented fluid volumes between microbubbles continuously deform and change their moving direction, leading to the “stretch and fold” of the fluid volume and thus rapid mixing of the to-be-mixed solutions, water and ink. At the exit of the mixing chamber, bubbles alternatively enter the channel,

recovering bubble-segmented flow. Complete mixing can be ensured by repeating this process using multiple mixing units.

Two control experiments were conducted to further demonstrate the enhanced mixing efficiency of the bubble-based chaotic mixer. Figure 2b shows a control experiment at the same experimental conditions as shown in Fig. 2a except that no nitrogen gas was supplied. In the absence of microbubbles, two fluids (water and ink) co-injected at the 1:1 flow rate ratio show a clear interface between water and ink with no significant mixing.

In addition, we notice the enhanced mixing effect has been observed within the bubble-segmented flow due to the counter-rotating recirculation vortices in moving aqueous slugs (Hosokawa et al. 1999). In order to demonstrate that the enhanced mixing is mainly due to the stretch and fold of the fluid volume in our case, we fabricated a similar device with no expansion chambers. Figure 2c shows the image of the bubble-segmented flow within a straight microchannel. Although slightly improved mixing was observed compared to the laminar flow in Fig. 2b (due to the recirculation flow in aqueous slug), the mixing performance is far poorer than the bubble chaotic mixer in Fig. 2a.

We further characterized the performance of the mixer at various flow conditions. The nitrogen pressure was adjusted to maintain the bubble size and filling ratio to be roughly constant for all the flow conditions. The device was tested at four different water/ink flow rates (0.8, 2.0, 4.0, and 8.0  $\mu\text{l}/\text{min}$ , respectively) and the mixing results are shown in Fig. 3a–d. In all the cases, we observed the progression of mixing while the to-be-mixed liquid solutions flowed through the mixing chamber. The Péclet numbers ( $Pe = (Uw/D)$ ) where  $U$  is the average liquid flow velocity,  $w = 80 \mu\text{m}$  is the width of the channel, and  $D$

**Fig. 2** Principle of the bubble-based chaotic mixer. **a** (From left to right) The formation of the bubble-segmented laminar flow between water and ink, the stretch and fold of the fluidic volume due to the bubble–fluid interaction in the mixing chamber, and fully mixed fluids. **b** The control experiment with a mixing chamber but no bubble. **c** The control experiment with bubbles but no mixing chamber. The water/ink flow rates were 0.2  $\mu\text{l}/\text{min}$  for **a–c**, and the gas pressures for **a** and **c** were 1 psi

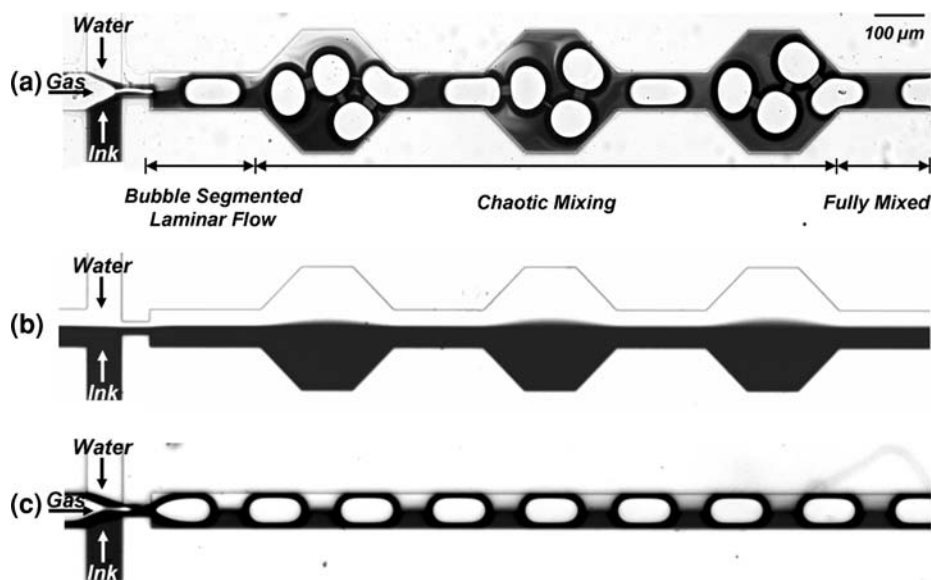
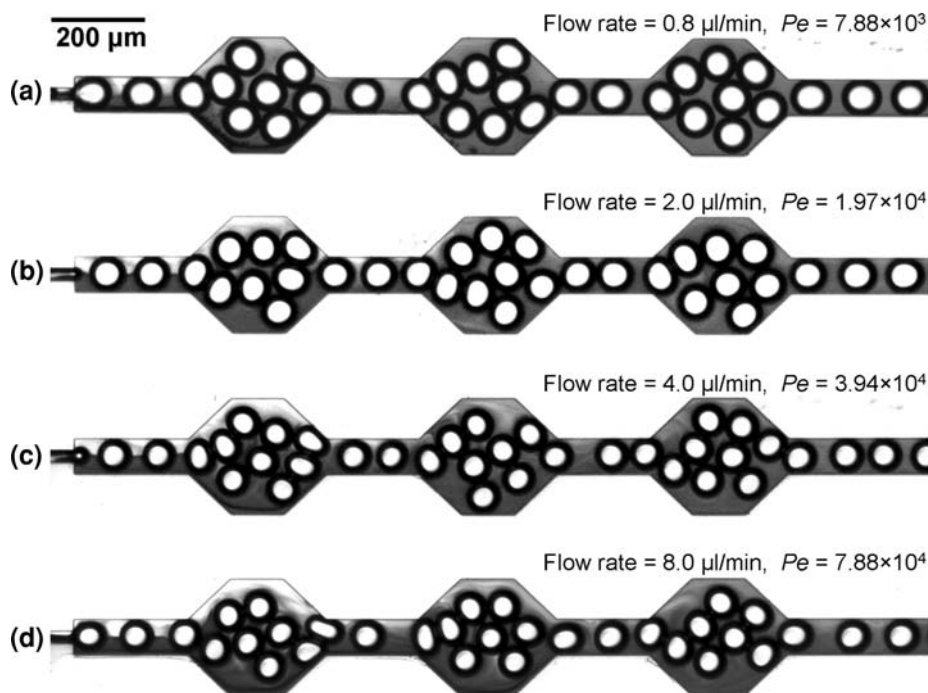


**Fig. 3** Experimental characterization of the chaotic bubble mixer. **a–d** Chaotic bubble mixer at different flow conditions. The water/ink injection flow rates and  $Pe$  were shown in the figure. The gas pressures for **a–d** were 3.0, 5.0, 6.5, and 9.0 psi, respectively



( $\sim 10^{-6}$  cm<sup>2</sup>/s) is the diffusivity of the ink (Garstecki et al. 2005), for these experiments were calculated to be  $7.88 \times 10^3$ ,  $1.97 \times 10^4$ ,  $3.94 \times 10^4$ , and  $7.88 \times 10^4$ , respectively. The high  $Pe$  suggests that in these experiments the advection of flow dominates over the diffusion. For a diffusion-only mixing (Mao et al. 2009b), a long mixing distance ( $d \sim Pe \times w > 10$  cm) would be required for complete homogenization of the fluids (Stroock et al. 2002). In chaotic mixing, however, it is expected that the mixing distance only increases logarithmically with  $Pe$ ,  $d \sim \lambda \ln(pe)$  (Stroock et al. 2002). In order to quantitatively characterize the progression of mixing along the channel length, we measured the mixing index ( $M$ ) of fluids at four different positions along the channel. The gray scale values (a good indicator of the ink concentration) of the fluids were sampled from the images in Fig. 3 at different locations (indicated as 1, 2, 3, and 4 in Fig. 4a), and the mixing index for each flow rate was calculated using the following equation:

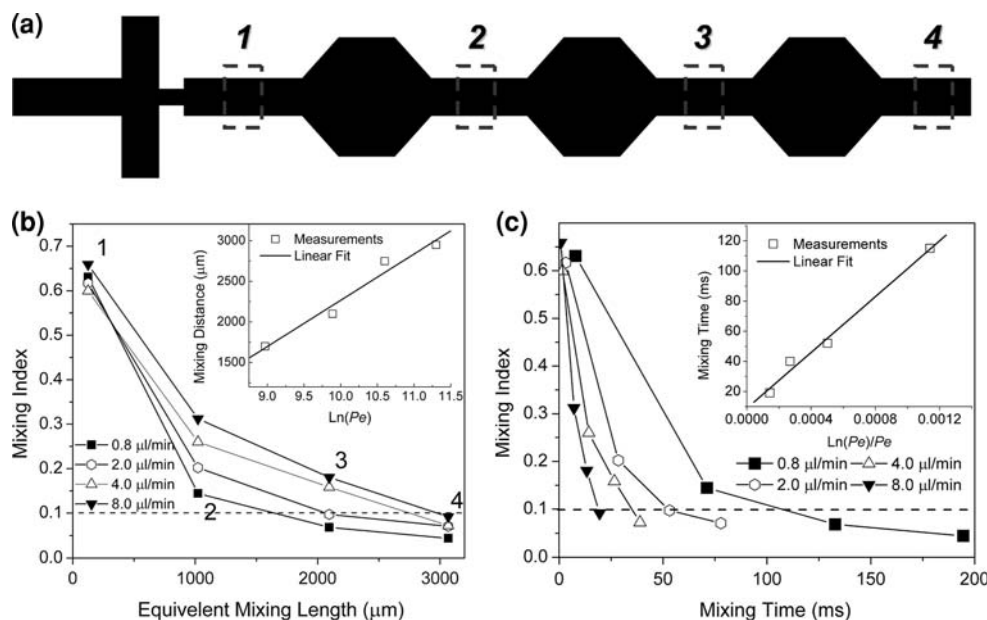
$$M = \sqrt{\frac{1}{n} \sum_{i=1}^n \left( \frac{I_i - I_m}{I_m} \right)^2},$$

where  $I_i$  is the gray scale value at a given point along the width of the channel,  $I_m$  is the average gray scale value, and  $n$  is the total number of sampled points (Garstecki et al. 2005, 2006). A mixing index value of 1.0 indicates completely separated solutions while a mixing index of 0.0 indicates completely mixed solutions. The mixing indices at different locations (positions 1–4) along the channel are shown in Fig. 4b. Because the width of the channel and

mixing chamber are different, we plotted the mixing index as the function of equivalent channel length (the volume of the fluid travelled divided by the channel cross-section area). We note that in Fig. 4b the mixing index decreases along the length of the mixer while fluids need to travel a longer distance for a complete mixing at higher  $Pe$ . We arbitrarily chose a threshold of 0.1 for acceptable mixing, and the mixing distance was defined as the equivalent mixing length the fluidic volume needs to travel to reach the mixing index of 0.1. The mixing distances were plotted as a function of  $\ln(Pe)$  in the inset of Fig. 4b and a linear relation was found, which agrees with the previous theoretical analysis and experimental observation (Stroock et al. 2002; Song et al. 2003) and suggests that in our chaotic bubble mixer the mixing distance increases logarithmically with  $Pe$ .

In Fig. 4c, we also plot the mixing index as a function of time for four different experiment conditions. The mixing indices were shown to rapidly decrease with the time. Similarly we defined the mixing time ( $t_{\text{mix}}$ ) as the time it takes for the mixing index to reach below 0.1. A scaling law of  $t_{\text{mix}} = \frac{d}{U} \sim \frac{\lambda \ln(pe)}{U} \sim \frac{\lambda w \ln(pe)}{D Pe} \sim \frac{\ln(pe)}{Pe}$  (Fig. 4c inset) was observed, which is also in good agreement with the theoretical analysis and experiment observation in the literatures (Ottino 1994; Song et al. 2003). At present, a minimum mixing time of  $\sim 20$  ms was achieved for water/ink flow rates of 8.0  $\mu\text{l}/\text{min}$  ( $Pe = 7.88 \times 10^4$ ) (Fig. 4c). However, the scaling law between the mixing time and  $Pe$  clearly indicated that the mixing time decreases with increasing  $Pe$ , suggesting that a faster mixing time (e.g., sub-millisecond mixing) can be potentially achieved

**Fig. 4** **a** Mixing index was sampled at different locations (positions 1–4) of the chaotic bubble mixer. **b** Plot of mixing index as a function of equivalent mixing length. *Inset:* The mixing distance was extracted and plotted against  $\text{Ln}(Pe)$ . **c** Plot of mixing index as a function of mixing time. *Inset:* The mixing time was extracted and plotted against  $\text{Ln}(Pe)/Pe$



with higher  $Pe$  or the further optimization of the channel geometry and other experimental conditions such as bubble size/bubble filling ratio.

Finally, we show that on completion of the the mixing, bubbles can be conveniently removed from the aqueous solution using a comb-shaped microfluidic structure (Günther et al. 2004). The comb-shaped structure includes an additional branch for extracted fluid and a series of capillarity channels which connect the branch with the main channel. The separation relied on the capillary force which prevents microbubbles from entering the separation channel. If the pressure difference across the capillary is less than the capillary pressure, then the segmented fluids between bubbles can be drawn from the capillary and separated from the gas. In Fig. 5, we observed that the mixed aqueous solution could travel through the narrow capillary channels and be extracted to the branch channel while the bubbles were prevented from entering the capillary channels, and remained in the main channel. Such a post-mixing bubble-extraction step is advantageous when

compared to droplet-based chaotic mixers if further sample purification and analyses are needed.

### 4 Conclusions

In this study, we have presented a novel, rapid microfluidic mixing technique, which generates complete mixing and homogenization of the fluids at fast rates by means of chaotic stretching and folding of segmented fluid between microbubbles. This mixing technique is simple to implement and exhibits promising mixing performance (mixing time  $\sim 20$  ms). Full potential of rapid mixing using bubbles, especially mixing in a few tens of milliseconds, has yet to be demonstrated in previous study. We believe that this device has great potential for a series of bio/chemical assays such as enzymatic kinetics and chemical synthesis where rapid mixing is needed.

**Acknowledgments** Authors thank Daniel Ahmed and Aitan Lawit for help in the manuscript preparation. This research was supported by National Science Foundation (ECCS-0824183 and ECCS-0801922) and the Penn State Center for Nanoscale Science (MRSEC). Components of this study were conducted at the Penn State node of the NSF-funded National Nanotechnology Infrastructure Network (NNIN).

### References

Biddiss E, Erickson D, Li D (2004) Heterogeneous surface charge enhanced micromixing for electrokinetic flows. *Anal Chem* 76:3208–3213  
 Chang CC, Yang RJ (2007) Electrokinetic mixing in microfluidic systems. *Microfluid Nanofluid* 3:501–525

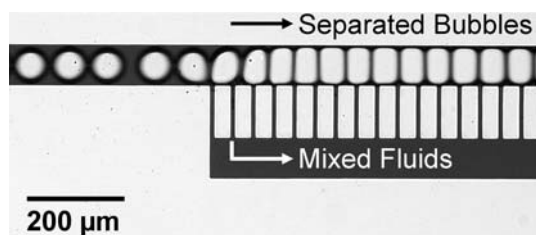


**Fig. 5** Separation of bubble after the mixing. The fully mixed fluids can be extracted through the “comb fingers,” or capillary channels to the branch channel while bubbles are retained in the main channel due to the surface tension

- de Mello J, de Mello A (2004) Focus microscale reactors: nanoscale products. *Lab Chip* 4:11N–15N
- Floyd-Smith TM, Golden JP, Howell PB, Ligler FS (2006) Characterization of passive microfluidic mixers fabricated using soft lithography. *Microfluid Nanofluid* 2:180
- Garstecki P, Fischbach MA, Whitesides GM (2005) Design for mixing using bubbles in branched microfluidic channels. *Appl Phys Lett* 86:244108
- Garstecki P, Fuerstman MJ, Fischbach MA, Sia SK, Whitesides GM (2006) Mixing with bubbles: a practical technology for use with portable microfluidic devices. *Lab Chip* 6:207–212
- Günther A, Khan SA, Thalmann M, Trachsel F, Jensen KF (2004) Transport and reaction in microscale segmented gas–liquid flow. *Lab Chip* 4:278–286
- Hardt S, Drese KS, Hessel V, Schönfeld F (2005) Passive micromixers for applications in the microreactor and  $\mu$ TAS fields. *Microfluid Nanofluid* 1:108
- Hosokawa K, Fujii T, Endo I (1999) Handling of picoliter liquid samples in a poly(dimethylsiloxane)-based microfluidic device. *Anal Chem* 71:4781–4785
- Kang T, Singh M, Kwon T, Anderson P (2008) Chaotic mixing using periodic and aperiodic sequences of mixing protocols in a micromixer. *Microfluid Nanofluid* 4:589–599
- Knight JB, Vishwanath A, Brody JP, Austin RH (1998) Hydrodynamic focusing on a silicon chip: mixing nanoliters in micro-seconds. *Phys Rev Lett* 80:3863–3866
- Liu RH, Stremmer MA, Sharp KV, Olsen MG, Santiago JG, Adrian RJ, Aref H, Beebe DJ (2000) Passive mixing in a three-dimensional serpentine microchannel. *J Microelectromech Syst* 9:190–197
- Mao X, Waldeisen JR, Huang TJ (2007a) “Microfluidic drifting”—implementing three-dimensional hydrodynamic focusing with a single-layer planar microfluidic device. *Lab Chip* 7:1260–1262
- Mao X, Waldeisen JR, Juluri BK, Huang TJ (2007b) Hydrodynamically tunable optofluidic cylindrical microlens. *Lab Chip* 7:1303–1308
- Mao X, Lin SS, Dong C, Huang TJ (2009a) Single-layer planar on-chip flow cytometer using microfluidic drifting based three-dimensional (3D) hydrodynamic focusing. *Lab Chip* 9:1583–1589
- Mao X, Lin SS, Lapsley MI, Shi J, Juluri BK, Huang TJ (2009b) Tunable liquid gradient refractive index (L-GRIN) lens with two degrees of freedom. *Lab Chip* 9:2050–2058
- Miller EM, Wheeler AR (2008) A digital microfluidic approach to homogeneous enzyme assays. *Anal Chem* 80:1614–1619
- Ottino JM (1989) The kinematics of mixing: stretching, chaos, and transport. Cambridge University Press, Cambridge
- Ottino JM (1994) Mixing and chemical reactions a tutorial. *Chem Eng Sci* 49:4005–4027
- Ottino JM, Wiggins S (2004) Designing optimal micromixers. *Science* 305:485–486
- Park HY, Qiu X, Rhoades E, Korlach J, Kwok LW, Zipfel WR, Webb WW, Pollack L (2006) Achieving uniform mixing in a microfluidic device: hydrodynamic focusing prior to mixing. *Anal Chem* 78:4465–4473
- Pollack L, Tate MW, Darnton NC, Knight JB, Gruner SM, Eaton WA, Austin RH (1999) Compactness of the denatured state of a fast-folding protein measured by submillisecond small-angle x-ray scattering. *Proc Natl Acad Sci USA* 96:10115–10117
- Puleo CM, Wang T-H (2009) Microfluidic means of achieving attomolar detection limits with molecular beacon probes. *Lab Chip*. doi:10.1039/b819605b
- Schönfeld F, Hessel V, Hofmann C (2004) An optimised split-and-recombine micro-mixer with uniform ‘chaotic’ mixing. *Lab Chip* 4:65–69
- Shi J, Mao X, Ahmed D, Colletti A, Huang TJ (2008) Focusing microparticles in a microfluidic channel with standing surface acoustic waves (SSAW). *Lab Chip* 8:221–223
- Song H, Ismagilov RF (2003) Millisecond kinetics on a microfluidic chip using nanoliters of reagents. *J Am Chem Soc* 125:14613–14619
- Song H, Bringer MR, Tice JD, Gerdtz CJ, Ismagilov RF (2003) Experimental test of scaling of mixing by chaotic advection in droplets moving through microfluidic channels. *Appl Phys Lett* 83:4664–4666
- Stroock AD, Dertinger SKW, Ajdari A, Mezic I, Stone HA, Whitesides GM (2002) Chaotic mixer for microchannels. *Science* 295:647–651
- Therriault D, White SR, Lewis JA (2003) Chaotic mixing in three-dimensional microvascular networks fabricated by direct-write assembly. *Nat Mater* 2:265–271
- Wu Z, Nguyen N-T (2005) Convective–diffusive transport in parallel lamination micromixers. *Microfluid Nanofluid* 1:208–217
- Yang J-T, Huang K-J, Lin Y-C (2005) Geometric effects on fluid mixing in passive grooved micromixers. *Lab Chip* 5:1140–1147